

6th International Conference on Signal and Image Processing (SIPRO 2020)

July 25-26, 2020, London, United Kingdom



DESIGN OF ACTIVE INDUCTOR AND STABILITY TEST FOR PASSIVE RLC LOW-PASS FILTERS

Minh Tri Tran*, Anna Kuwana,
Haruo Kobayashi



1. Research Background

- **Reviews of Complex Functions**
- **Transfer Function and Its Self-loop Function**
- **Limitations of Conventional Methods**

2. Analysis of High-Order Transfer Functions

- **Behaviors of High-order Passive Transmission Spaces**
- **Numerical Examples and Design of Active Inductor**

3. Experimental Results

- **Measurements of Self-loop Functions in RLC networks**
- **Operating region of Active Serial RLC Low-pass Filter**

4. Conclusions

1. Research Background

Motivation of Study

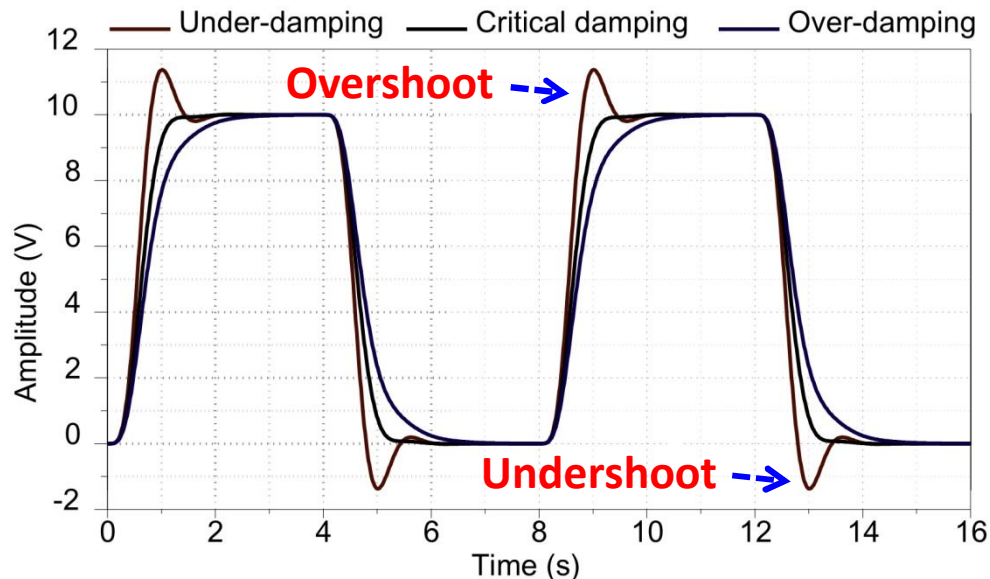
Large overshoots + ringing + unwanted voltage transients

→ **Damped oscillation noise**

→ **Unstable system**



STABILITY TEST



○ Ringing occurs in both **with** and **without** feedback systems.

○ Ringing affects both **input** and **output** signals.

1. Research Background

Objectives and Achievements

Objectives

- Investigation of operating region of high-order systems in both time and frequency domains
 - Over-damping (high delay in rising time)
 - Critical damping (max power propagation)
 - **Under-damping** (overshoot and ringing)

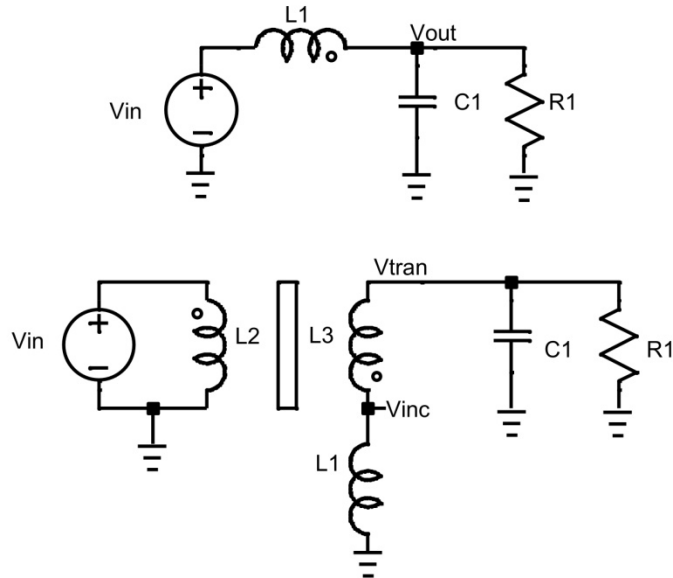
Achievements

- Design of active inductor and measurement of self-loop function in active serial RLC LPF

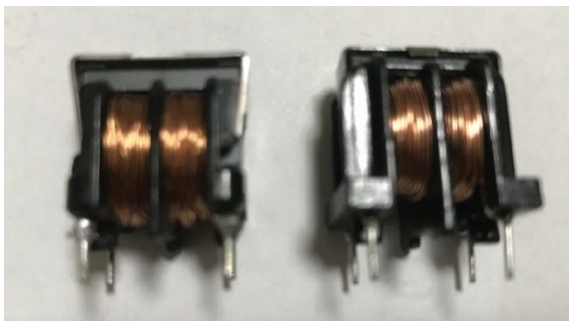
1. Research Background

Approaching Methods

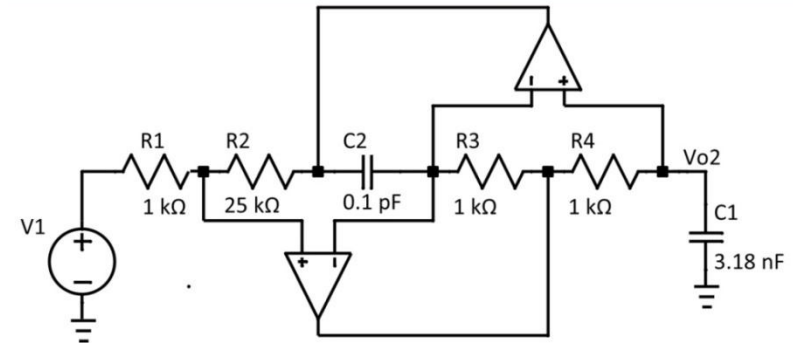
Passive RLC Low-pass Filter



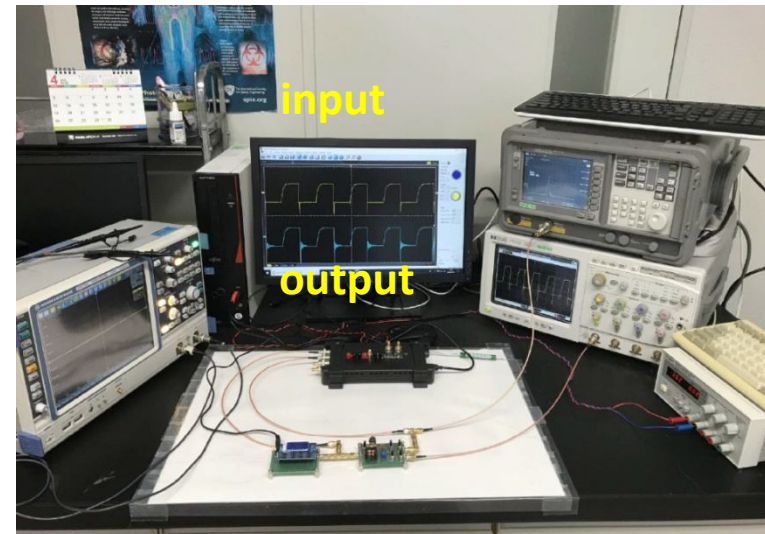
Balun transformer



Active RLC Low-pass Filter



Implementation of active RLC LPF



1. Research Background

Reviews of Complex Functions

Complex function with frequency variable

$$H(\omega) = \text{Re}(\omega) + j\text{Im}(\omega) = \text{Real}\{H(\omega)\} + j\text{Imag}\{H(\omega)\}$$

In complex plane domain

$$H(\omega) = \begin{cases} \text{Re}(\omega) = \text{Real}\{H(\omega)\} \\ \text{Im}(\omega) = \text{Imag}\{H(\omega)\} \\ \text{Fre}(\omega) = \textit{angular frequency} \end{cases}$$

In spectrum domain

$$H(\omega) = |H(\omega)|e^{j\theta(\omega)}$$

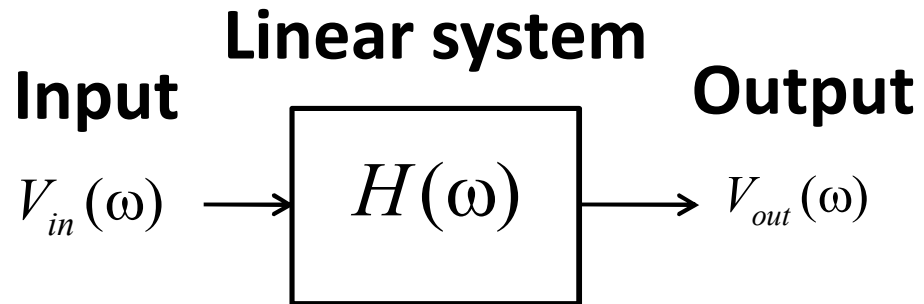
$$|H(\omega)| = \sqrt{[\text{Re}\{H(\omega)\}]^2 + [\text{Im}\{H(\omega)\}]^2}$$

$$\theta(\omega) = \arctan\left(\frac{\text{Im}\{H(\omega)\}}{\text{Re}\{H(\omega)\}}\right)$$

- Polar chart (**Nyquist chart**)
- Magnitude-frequency, angular-frequency plots (**Bode plots**)
- Magnitude-angular diagrams (**Nicholas diagrams**)

1. Research Background

Transfer Function and Its Self-loop Function



$A(\omega)$: Open loop function

$H(\omega)$: Transfer function

$L(\omega)$: Self-loop function

Transfer function

$$H(\omega) = \frac{V_{out}(\omega)}{V_{in}(\omega)} = \frac{A(\omega)}{1 + L(\omega)}$$



$$H(\omega) = \frac{A(\omega)}{0} = \infty$$

Unstable system

Constraint for oscillation

$$1 + L(\omega) = 0 \Rightarrow \begin{cases} |L(\omega)| = 1 \\ \angle L(\omega) = -180^\circ \end{cases}$$



**PHASE MARGIN
AT UNITY GAIN**

1. Research Background

Signal Flow Graph for Transfer Function

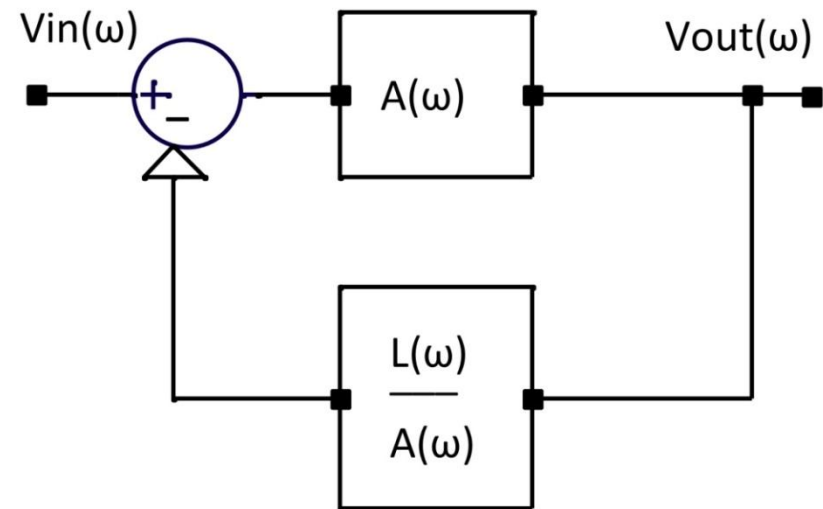
Transfer function

$$H(\omega) = \frac{V_{out}(\omega)}{V_{in}(\omega)} = \frac{A(\omega)}{1 + L(\omega)}$$

Output voltage

$$V_{out}(\omega) = A(\omega) \left[V_{in}(\omega) - \frac{L(\omega)}{A(\omega)} V_{out}(\omega) \right]$$

Negative feedback Network



Signal flow graph

To meet the specified requirements

- High stability
- Fast transient response, and
- Good steady-state performance.



STABILITY TEST

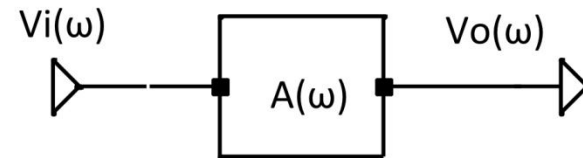
1. Research Background

Proposed Comparison Measurement Technique

Open loop function

Step1:

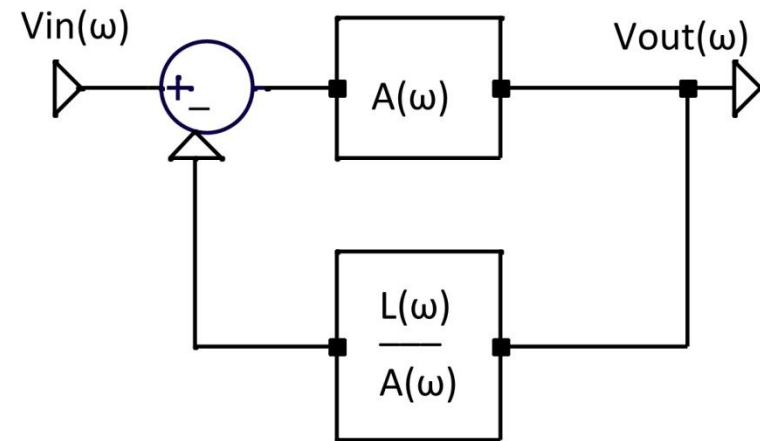
$$A(\omega) = \frac{V_i(\omega)}{V_o(\omega)}$$



Transfer function

Step2:

$$H(\omega) = \frac{V_{out}(\omega)}{V_{in}(\omega)} = \frac{A(\omega)}{1 + L(\omega)}$$



Self-loop function

Step3:

$$L(\omega) = \frac{A(\omega)}{H(\omega)} - 1$$

Sequence of steps:

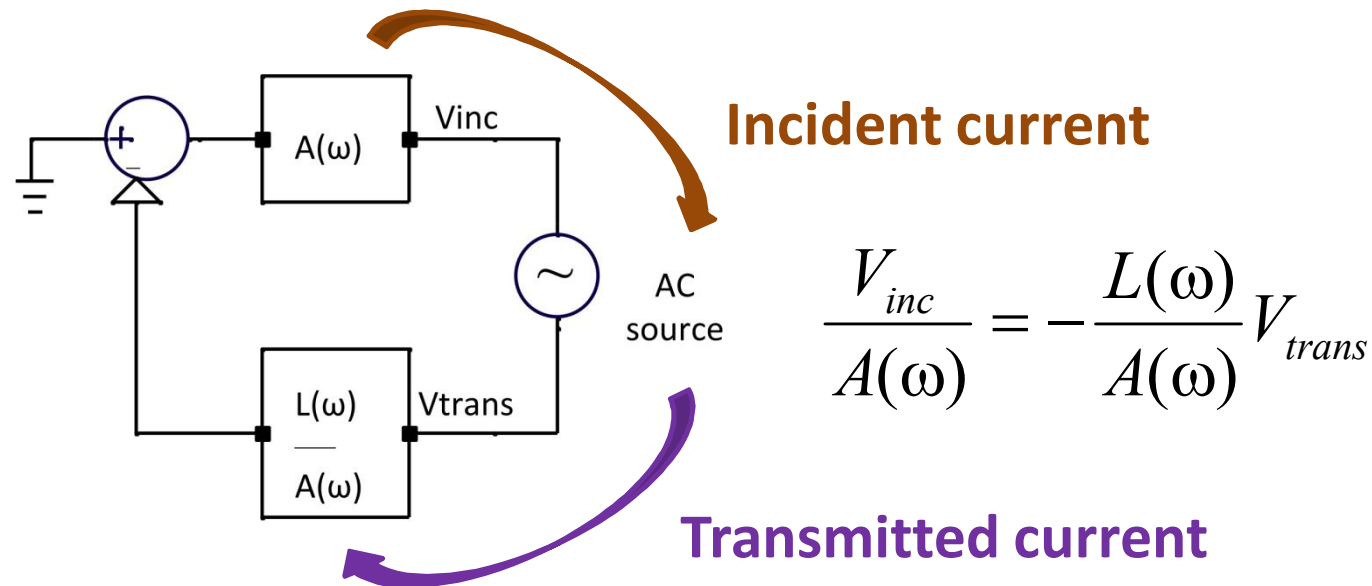
- (i) Measurement of **open loop function** $A(\omega)$,
- (ii) Measurement of **transfer function** $H(\omega)$, and
- (iii) Derivation of **self-loop function**.

1. Research Background

Proposed Alternating Current Conservation (1)

Idea: Alternating current is conserved.

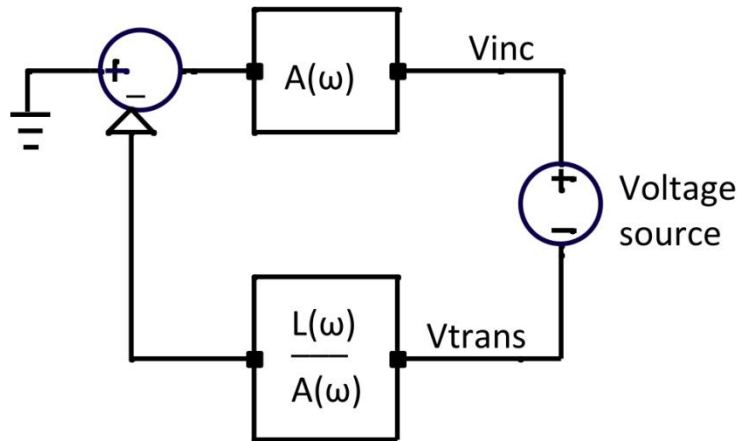
Incident current = Transmitted current



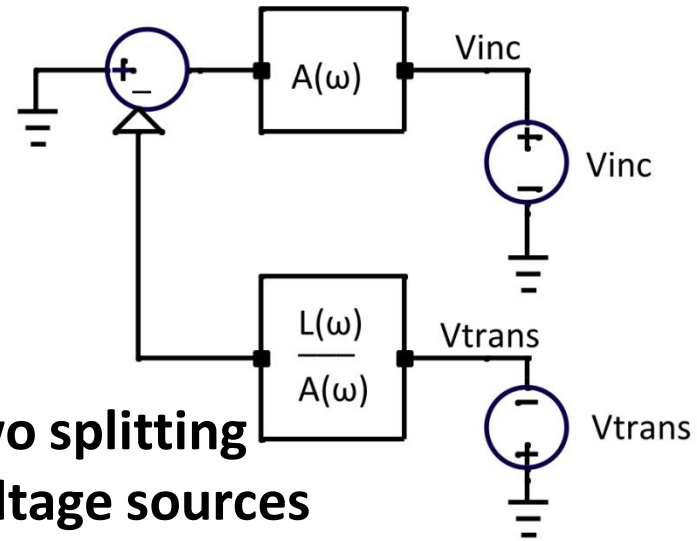
Self-loop function: $L(\omega) = -\frac{V_{inc}}{V_{trans}}$

1. Research Background

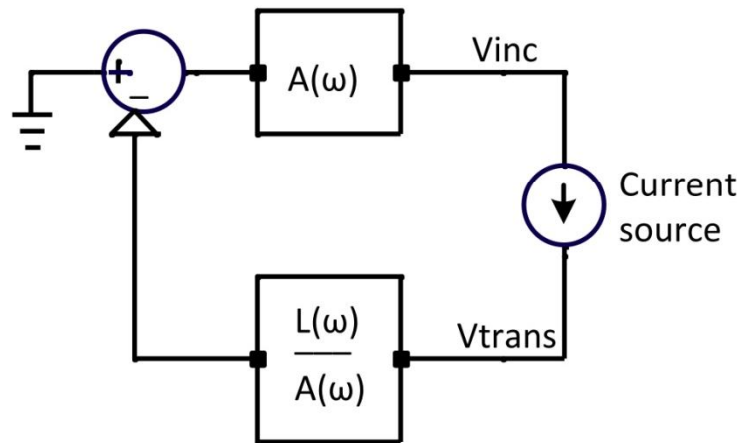
Proposed Alternating Current Conservation (2)



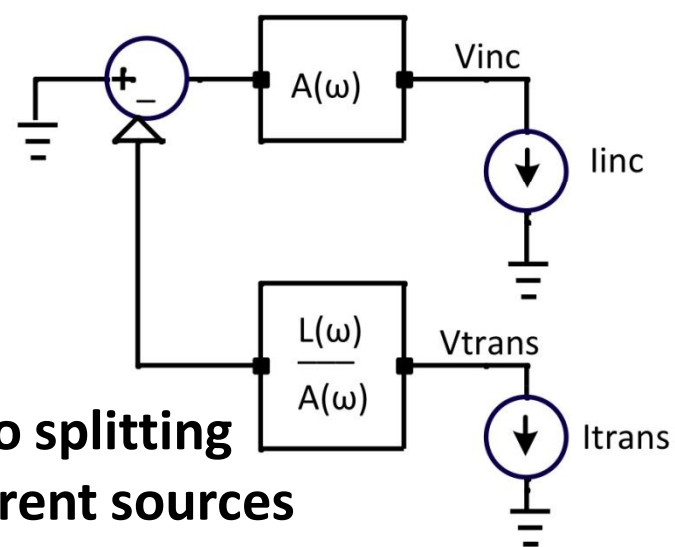
One voltage source



Two splitting voltage sources



One current source

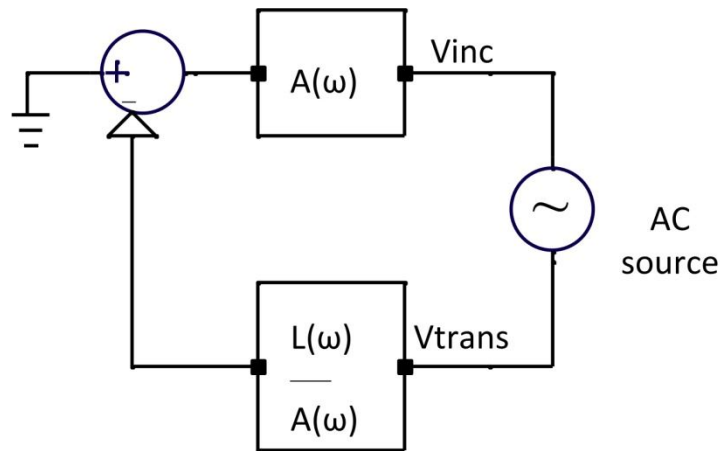


Two splitting current sources

1. Research Background

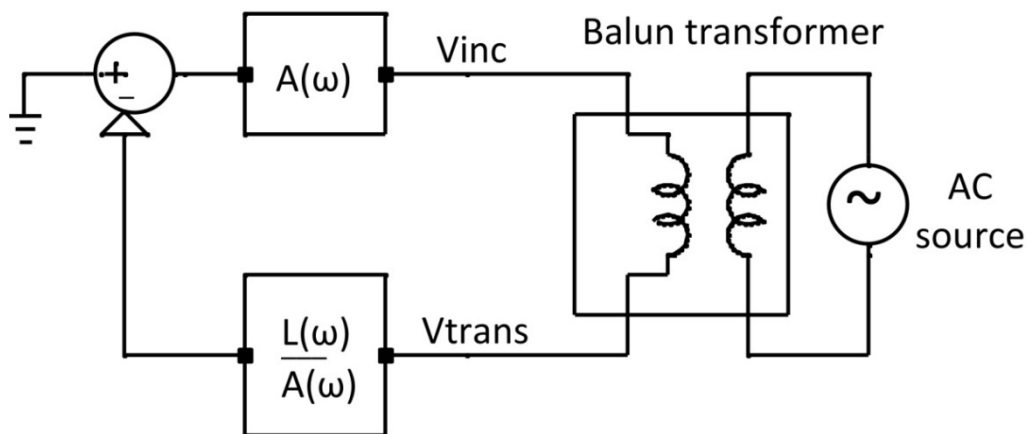
Proposed Alternating Current Conservation (3)

Alternating current conservation using **balun transformer**

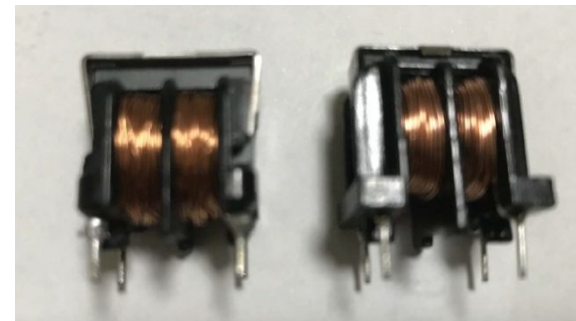


Self-loop function:

$$L(\omega) = -\frac{V_{inc}}{V_{trans}}$$



**Balun transformer
(10 mH inductance)**



1. Research Background

Proposed Widened Superposition Principle

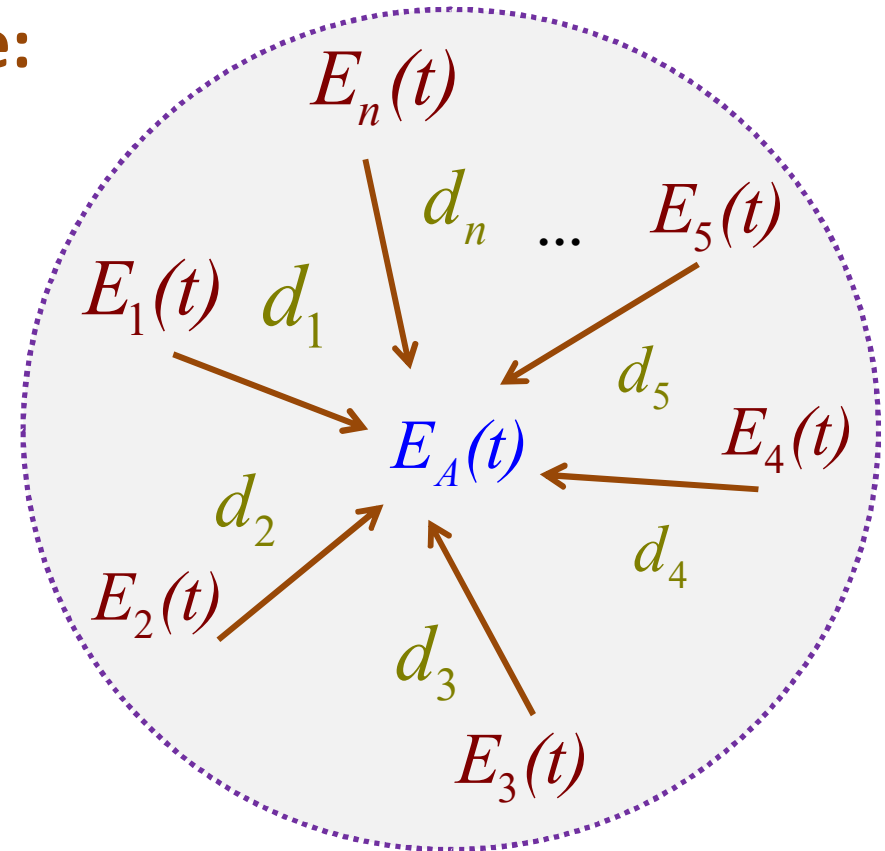
Widened Superposition Principle:

$$E_A(t) \sum_{i=1}^n \frac{1}{d_i} = \sum_{i=1}^n \frac{E_i(t)}{d_i}$$

$E_A(t)$: *Energy at one place*

$E_i(t)$: *Input sources*

$d_i(t)$: *Resistance distances*



- Multi-source systems, feedback networks (op amps, amplifiers), polyphase filters, complex filters...

1. Research Background

Limitations of Conventional Methods (1)

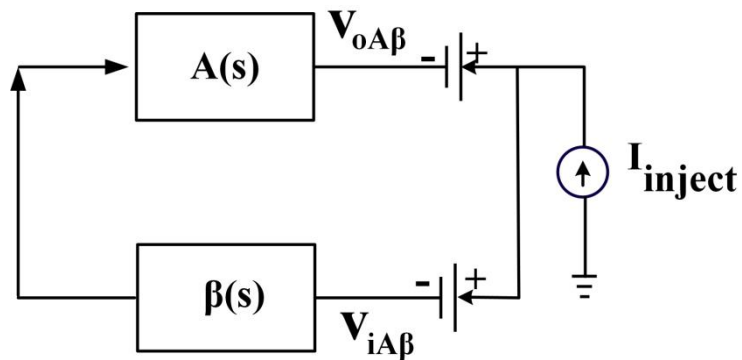
[7] Middlebrook, R.D., "Measurement of Loop Gain in Feedback Systems", Int. J. Electronics, vol 38, No. 4, pp. 485-512, 1975.

Measurement of loop gain

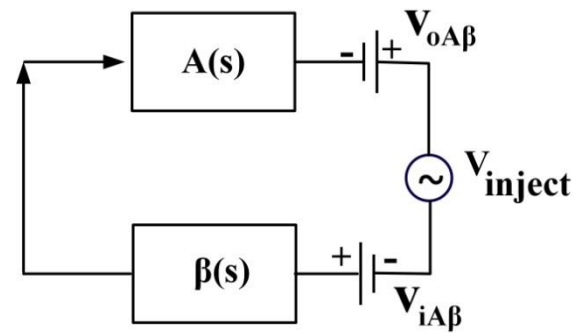
❖ Current injection

❖ Voltage injection

$$L(\omega) = \frac{V_{oA\beta}(\omega)}{v_{iA\beta}(\omega)}$$



Current injection method



Voltage injection method

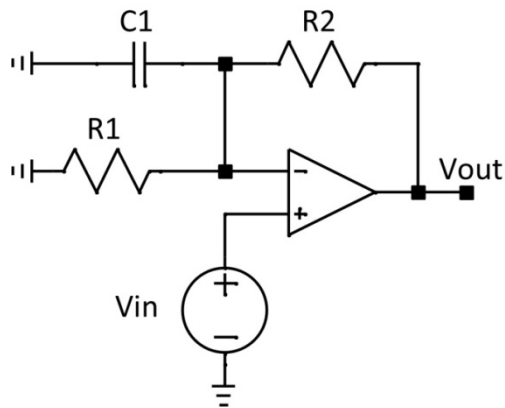
→ **Difficult** to measure self-loop function in analog circuits

1. Research Background

Limitations of Conventional Methods (2)

[9] A. S. Sedra and K. C. Smith, "Microelectronic Circuits," 6th ed. Oxford University Press, New York, 2010.

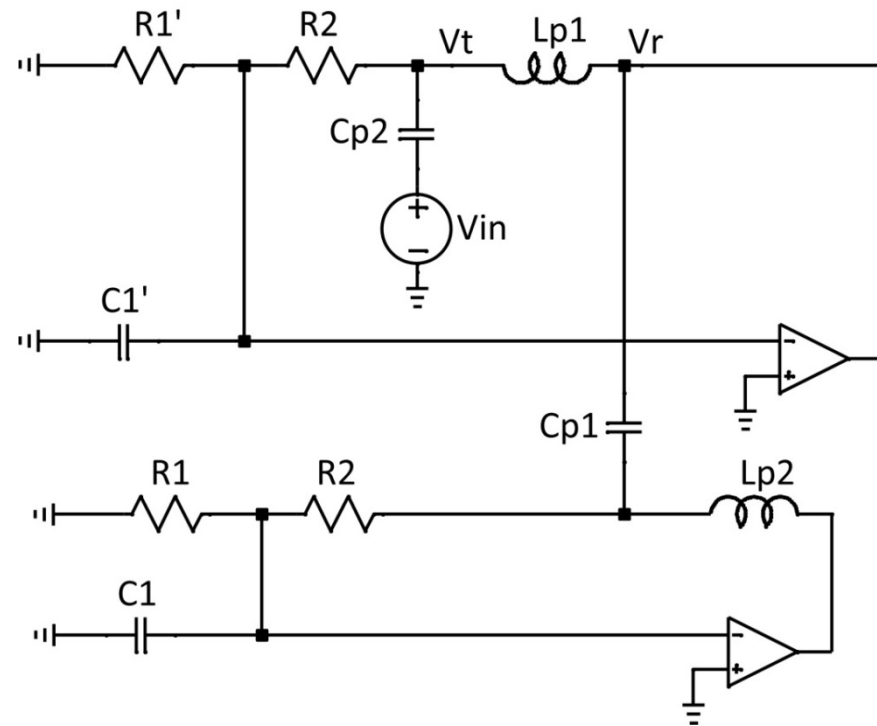
Measurement of loop gain



$$L(\omega) = \frac{V_r(\omega)}{V_t(\omega)}$$



❖ Replica measurement



→ **Difficult** to measure two real different circuits

1. Research Background

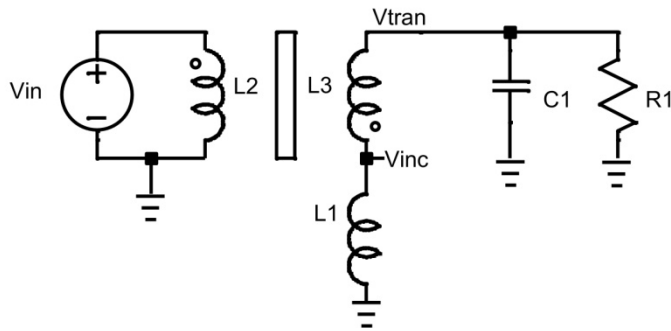
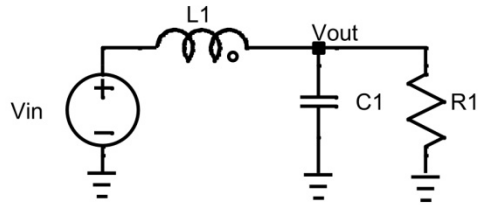
Limitations of Conventional Methods (3)

- **Conventional Superposition:**
 - Solving for every source voltage and current, perhaps several times.
- **Conventional measurement of loop gain (Middle Brook's)**
 - Applying only in feedback systems (switching DC-DC converters).
- **Conventional replica measurement of loop gain**
 - Using two identical networks (difficult in practical measurement).
- **Conventional Nyquist's stability condition**
 - Using in theoretical analysis for feedback systems (Lab simulation).
- **Conventional concepts, analysis and measurement of loop gain are not unique.**

2. Analysis of High-Order Transfer Functions

Second-order Parallel RLC Low-pass Filter

Parallel RLC low-pass filter



Apply superposition principle at V_{out}

$$V_{out} \left(\frac{1}{R} + \frac{1}{Z_C} + \frac{1}{Z_L} \right) = \frac{V_{in}}{Z_L};$$

Transfer function & self-loop function:

$$H(\omega) = \frac{V_{out}}{V_{in}} = \frac{1}{1 + a_0 (j\omega)^2 + a_1 j\omega};$$

$$L(\omega) = a_0 (j\omega)^2 + a_1 j\omega;$$

Where:

$$a_0 = LC; \quad a_1 = \frac{L}{R};$$

$$\omega_0 = 1/\sqrt{LC};$$

$$|Z_L| = \omega_0 L; \quad |Z_C| = 1/\omega_0 C;$$

Operating regions

• **Over-damping:** $\frac{1}{LC} < \left(\frac{R}{2L} \right)^2 \Leftrightarrow |Z_L| = |Z_C| < R/2$

• **Critical damping:** $\frac{1}{LC} = \left(\frac{R}{2L} \right)^2 \Leftrightarrow |Z_L| = |Z_C| = R/2$

• **Under-damping:** $\frac{1}{LC} > \left(\frac{R}{2L} \right)^2 \Leftrightarrow |Z_L| = |Z_C| > R/2$

2. Analysis of High-Order Transfer Functions

Behaviors of Second-order Transfer Function

Second-order transfer function:
$$H(\omega) = \frac{1}{1 + a_0(j\omega)^2 + a_1j\omega}$$

Case	Over-damped	Critically damped	Under-damped
Delta (Δ)	$\frac{1}{a_0} < \left(\frac{a_1}{2a_0}\right)^2 \Rightarrow \Delta = a_1^2 - 4a_0 > 0$	$\frac{1}{a_0} = \left(\frac{a_1}{2a_0}\right)^2 \Rightarrow \Delta = a_1^2 - 4a_0 = 0$	$\frac{1}{a_0} > \left(\frac{a_1}{2a_0}\right)^2 \Rightarrow \Delta = a_1^2 - 4a_0 < 0$
Module $ H(\omega) $	$\frac{1}{a_0} \sqrt{\omega^2 + \left(\frac{a_1}{2a_0} - \sqrt{\left(\frac{a_1}{2a_0}\right)^2 - \frac{1}{a_0}}\right)^2} \sqrt{\omega^2 + \left(\frac{a_1}{2a_0} + \sqrt{\left(\frac{a_1}{2a_0}\right)^2 - \frac{1}{a_0}}\right)^2}$	$\frac{1}{a_0} \sqrt{\omega^2 + \left(\frac{a_1}{2a_0}\right)^2}$	$\frac{1}{a_0} \sqrt{\left(\omega - \sqrt{\frac{1}{a_0} - \left(\frac{a_1}{2a_0}\right)^2}\right)^2 + \left(\frac{a_1}{2a_0}\right)^2} \sqrt{\left(\omega + \sqrt{\frac{1}{a_0} - \left(\frac{a_1}{2a_0}\right)^2}\right)^2 + \left(\frac{a_1}{2a_0}\right)^2}$
Angular $\theta(\omega)$	$-\arctan\left(\frac{\omega}{\frac{a_1}{2a_0} - \sqrt{\left(\frac{a_1}{2a_0}\right)^2 - \frac{1}{a_0}}}\right) - \arctan\left(\frac{\omega}{\frac{a_1}{2a_0} + \sqrt{\left(\frac{a_1}{2a_0}\right)^2 - \frac{1}{a_0}}}\right)$	$-2 \arctan\left(\frac{2a_0\omega}{a_1}\right)$	$-\arctan\left(\frac{\omega - \sqrt{\frac{1}{a_0} - \left(\frac{a_1}{2a_0}\right)^2}}{\frac{a_1}{2a_0}}\right) - \arctan\left(\frac{\omega + \sqrt{\frac{1}{a_0} - \left(\frac{a_1}{2a_0}\right)^2}}{\frac{a_1}{2a_0}}\right)$
$\omega_{cut} = \frac{a_1}{2a_0}$	$ H(\omega_{cut}) < \frac{2a_0}{a_1}$ $\theta(\omega_{cut}) > -\frac{\pi}{2}$	$ H(\omega_{cut}) = \frac{2a_0}{a_1}$ $\theta(\omega_{cut}) = -\frac{\pi}{2}$	$ H(\omega_{cut}) > \frac{2a_0}{a_1}$ $\theta(\omega_{cut}) < -\frac{\pi}{2}$

2. Analysis of High-Order Transfer Functions

Example of Second-order Transfer Function

Magnitude of transfer function

$$H_1(\omega) = \frac{1}{(j\omega)^2 + j\omega + 1} \Rightarrow |H_1(\omega)| = \frac{1}{\sqrt{\left(\omega - \frac{\sqrt{3}}{2}\right)^2 + \frac{1}{4}} \sqrt{\left(\omega + \frac{\sqrt{3}}{2}\right)^2 + \frac{1}{4}}}$$

• **Under-damping:**

$$\frac{\sqrt{3}-1}{2} < \omega < \frac{\sqrt{3}+1}{2} \Rightarrow |H_1(\omega)| > 1 \quad \left(\omega_1 = \frac{\sqrt{3}-1}{2} < \omega_{cut} = 1 \right)$$

• **Critical damping:**

$$H_2(\omega) = \frac{1}{(j\omega)^2 + 2j\omega + 1} \Rightarrow |H_2(\omega)| = \frac{1}{\omega^2 + 1} \quad (\omega_{cut} = 1)$$

• **Over-damping:**

$$H_3(\omega) = \frac{1}{(j\omega)^2 + 3j\omega + 1} \Rightarrow |H_3(\omega)| = \frac{1}{\sqrt{\omega^2 + \left(\frac{3-\sqrt{5}}{2}\right)^2} \sqrt{\omega^2 + \left(\frac{3+\sqrt{5}}{2}\right)^2}}$$

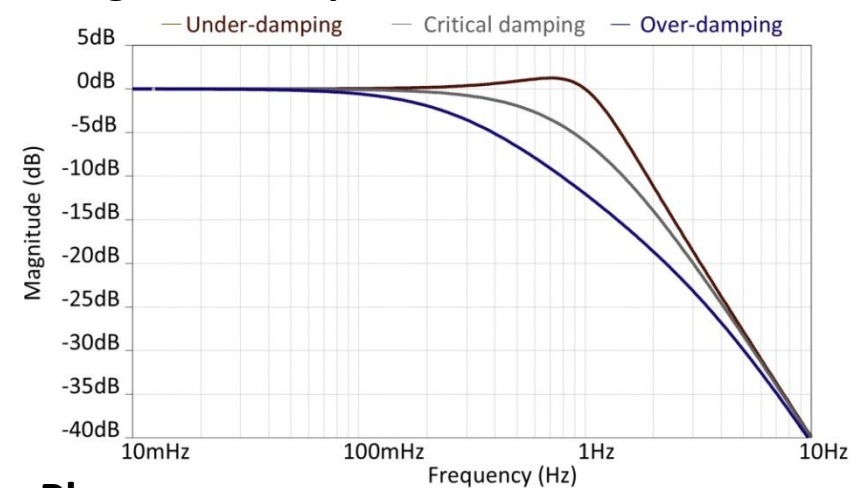
$$\frac{3-\sqrt{5}}{2} < \omega < \frac{3+\sqrt{5}}{2} \Rightarrow |H_3(\omega)| < 1 \quad \left(\omega_1 = \frac{3-\sqrt{5}}{2} < \omega_{cut} = 1 \right)$$

2. Analysis of High-Order Transfer Functions

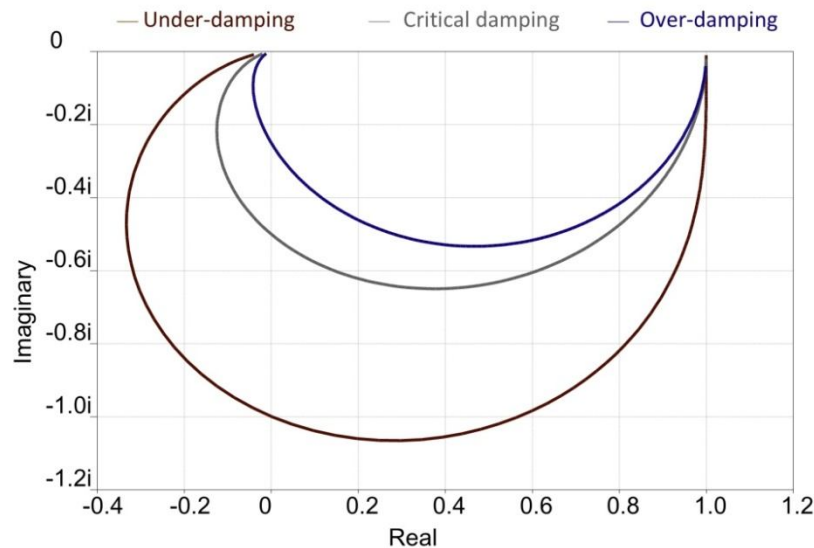
Simulations of Second-order Transfer Function

- **Under-damping:** $H_1(\omega) = \frac{1}{(j\omega)^2 + j\omega + 1}$;
- **Critical damping:** $H_2(\omega) = \frac{1}{(j\omega)^2 + 2j\omega + 1}$;
- **Over-damping:** $H_3(\omega) = \frac{1}{(j\omega)^2 + 3j\omega + 1}$;

Magnitude response

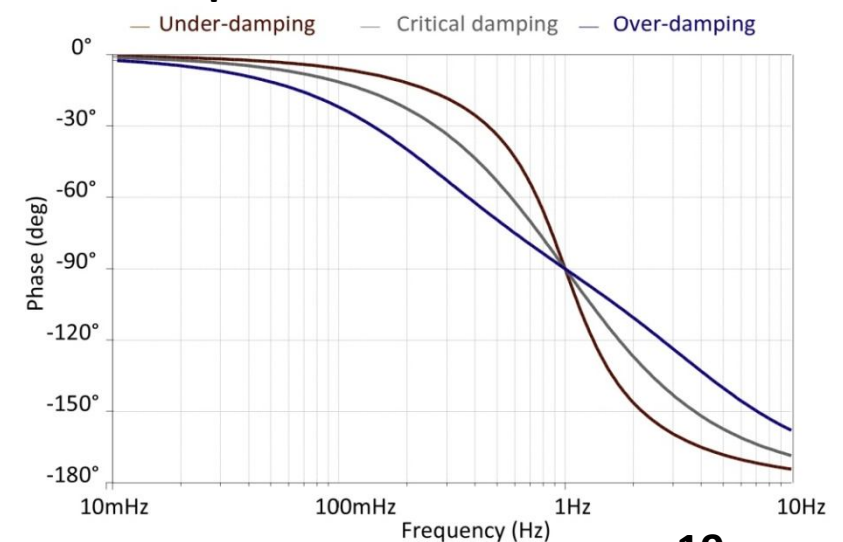


Polar chart of transfer function



Nyquist chart

Phase response



2. Analysis of High-Order Transfer Functions

Behaviors of Second-order Self-loop Function

Second-order self-loop function: $L(\omega) = j\omega[a_0 j\omega + a_1]$

Case	Over-damped	Critically damped	Under-damped
Delta (Δ)	$\Delta = a_1^2 - 4a_0 > 0$	$\Delta = a_1^2 - 4a_0 = 0$	$\Delta = a_1^2 - 4a_0 < 0$
$ L(\omega) $	$\omega\sqrt{(a_0\omega)^2 + a_1^2}$	$\omega\sqrt{(a_0\omega)^2 + a_1^2}$	$\omega\sqrt{(a_0\omega)^2 + a_1^2}$
$\theta(\omega)$	$\frac{\pi}{2} + \arctan \frac{a_0\omega}{a_1}$	$\frac{\pi}{2} + \arctan \frac{a_0\omega}{a_1}$	$\frac{\pi}{2} + \arctan \frac{a_0\omega}{a_1}$
$\omega_1 = \frac{a_1}{2a_0}\sqrt{\sqrt{5}-2}$	$ L(\omega_1) > 1$	$\pi - \theta(\omega_1) > 76.3^\circ$	$ L(\omega_1) < 1$
$\omega_2 = \frac{a_1}{2a_0}$	$ L(\omega_2) > \sqrt{5}$	$\pi - \theta(\omega_2) > 63.4^\circ$	$ L(\omega_2) < \sqrt{5}$
$\omega_3 = \frac{a_1}{a_0}$	$ L(\omega_3) > 4\sqrt{2}$	$\pi - \theta(\omega_3) > 45^\circ$	$ L(\omega_3) < 4\sqrt{2}$

2. Analysis of High-Order Transfer Functions

Behaviors of Second-order Self-loop Function

Second-order self-loop function: $L(\omega) = j\omega[a_0 j\omega + a_1]$

Unity gain of self-loop function $|L(\omega)| = \omega\sqrt{(a_0\omega)^2 + a_1^2} = 1$

Angular frequency at unity gain $\omega_1 = \frac{a_1}{2a_0}\sqrt{\sqrt{5}-2}$

Phase margin at unity gain of self-loop function

• **Under-damping:** Phase margin = $\pi - \theta(\omega_1) < 76.3^\circ$

• **Critical damping:** Phase margin = $\pi - \theta(\omega_1) = 76.3^\circ$

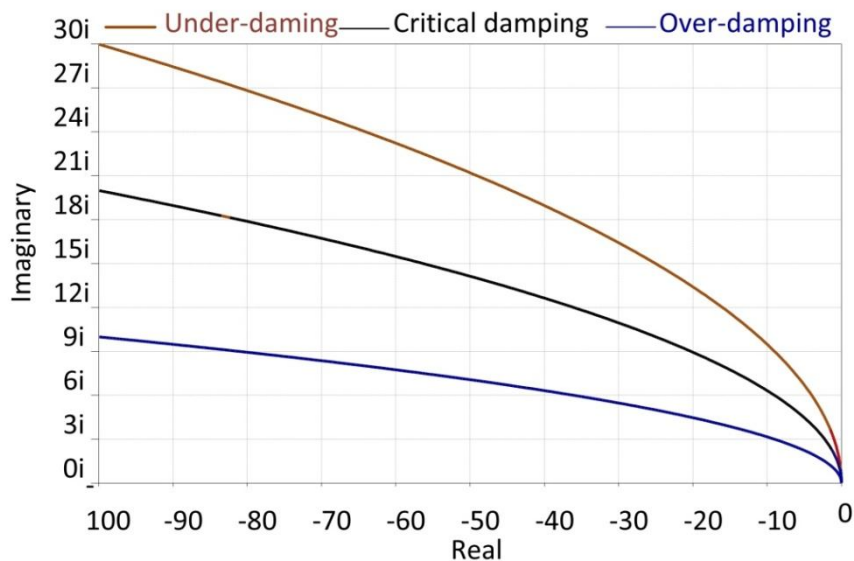
• **Over-damping:** Phase margin = $\pi - \theta(\omega_1) > 76.3^\circ$

2. Analysis of High-Order Transfer Functions

Simulations of Second-order Self-loop Function

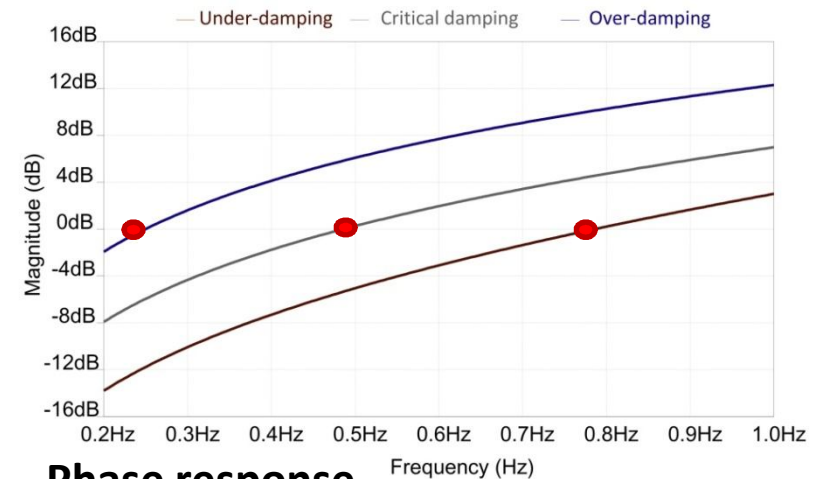
- **Under-damping:** $L_1(\omega) = (j\omega)^2 + j\omega;$
- **Critical damping:** $L_2(\omega) = (j\omega)^2 + 2j\omega;$
- **Over-damping:** $L_3(\omega) = (j\omega)^2 + 3j\omega;$

Polar chart of self-loop function

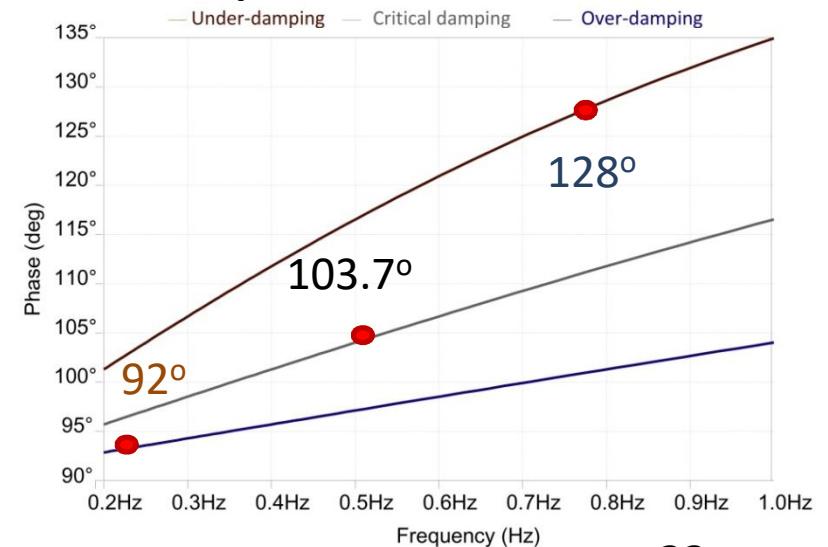


Nyquist chart

Magnitude response



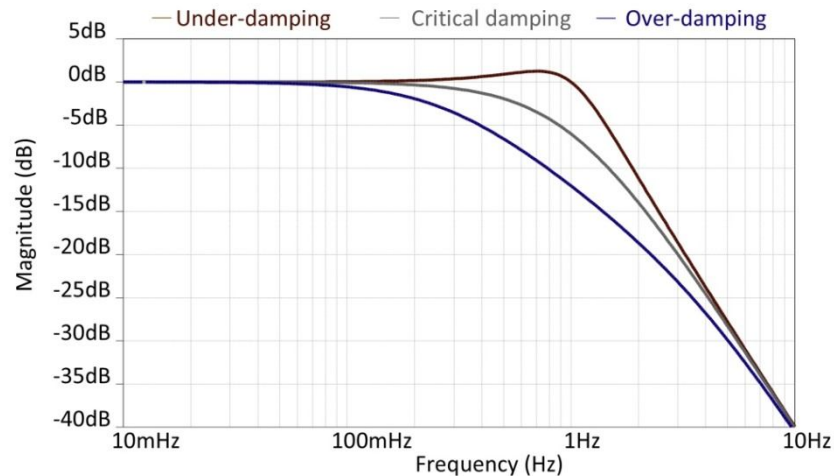
Phase response



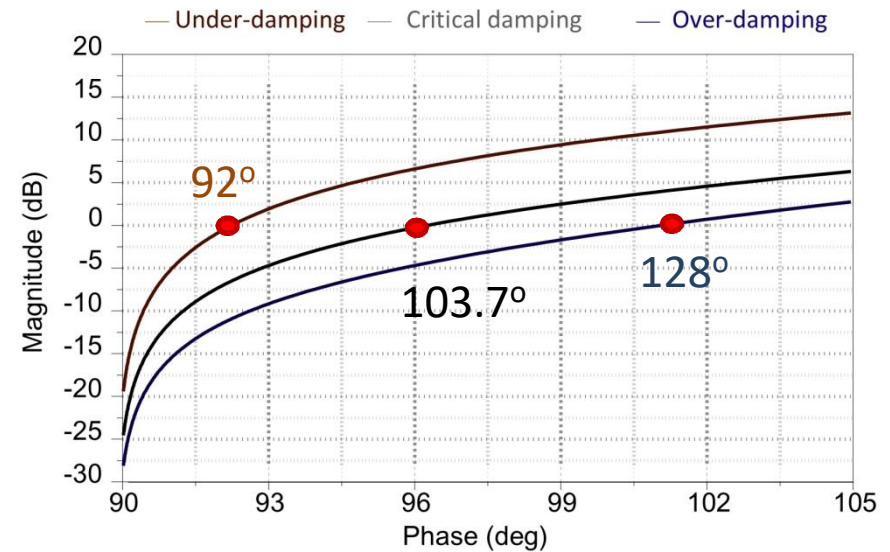
2. Analysis of High-Order Transfer Functions

Summary of Second-order System

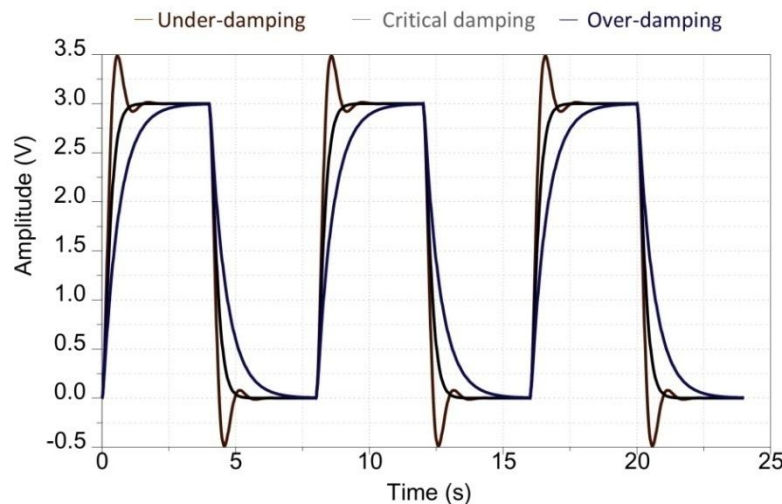
Magnitude response of transfer function



Magnitude-angular response of self-loop function



Transient response



Over-damping:

→ Phase margin is 88 degrees.

Critical damping:

→ Phase margin is 76.3 degrees.

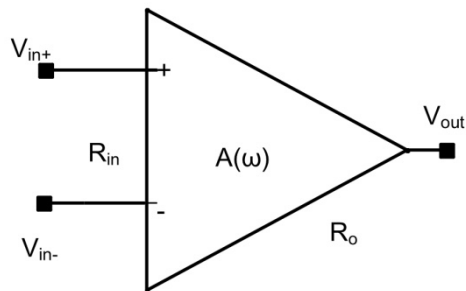
Under-damping:

→ Phase margin is 52 degrees.

2. Analysis of High-Order Transfer Functions

Mathematical Model of Ideal Op Amp

Ideal op amp



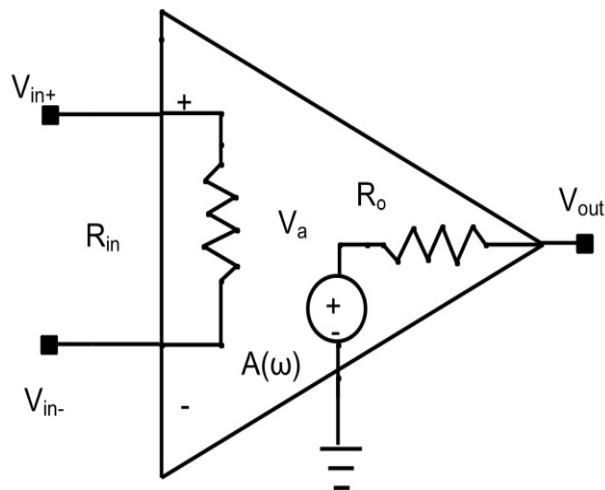
Open-loop function $A(\omega)$ of op amp

$$A(\omega) = \frac{V_{out}}{V_{in+} - V_{in-}} = \frac{A_0}{1 + \frac{j\omega}{\omega_{bw}}}$$

Gain-bandwidth (GBW), bandwidth fbw

$$GBW = A_0 f_{bw} \Rightarrow f_{bw} = \frac{GBW}{A_0}$$

Equivalent model of op amp



Here, GBW = 10 MHz, DC gain $A_0 = 100000$

Open-loop function and self-loop function

$$A(\omega) = \frac{10^5}{1 + j \frac{\omega}{200\pi}} ; L(\omega) = j \frac{\omega}{200\pi} = 10^5 \frac{V_{in}}{V_{out}} - 1$$

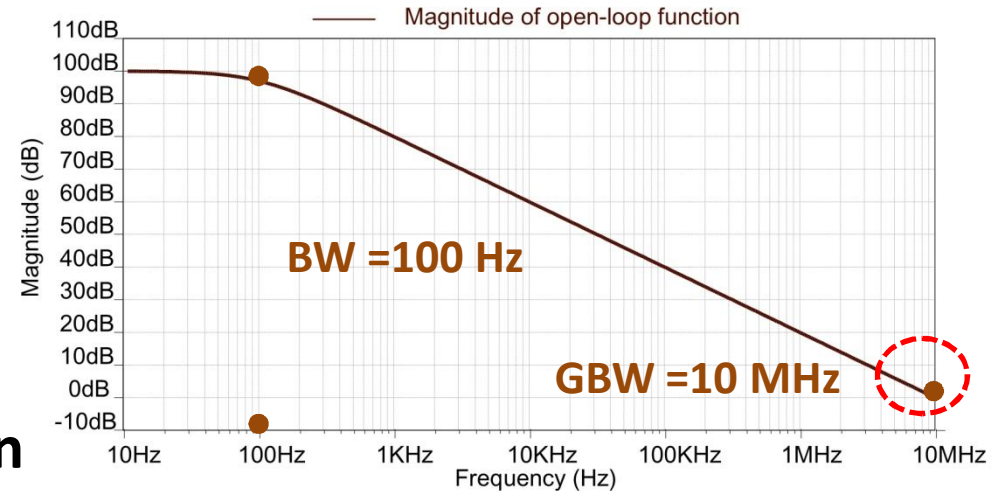
2. Analysis of High-Order Transfer Functions

Behavior of Open-loop Function of Ideal Op Amp

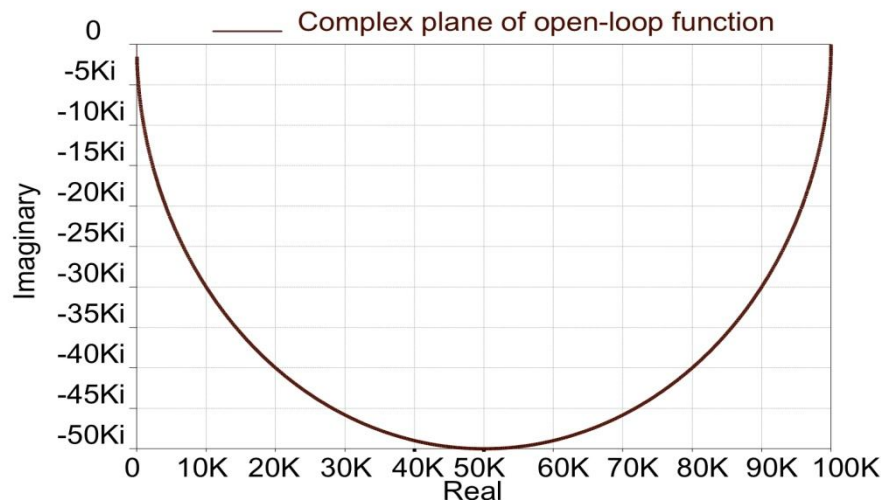
Open-loop function $A(\omega)$

$$A(\omega) = \frac{10^5}{1 + j \frac{\omega}{200\pi}}$$

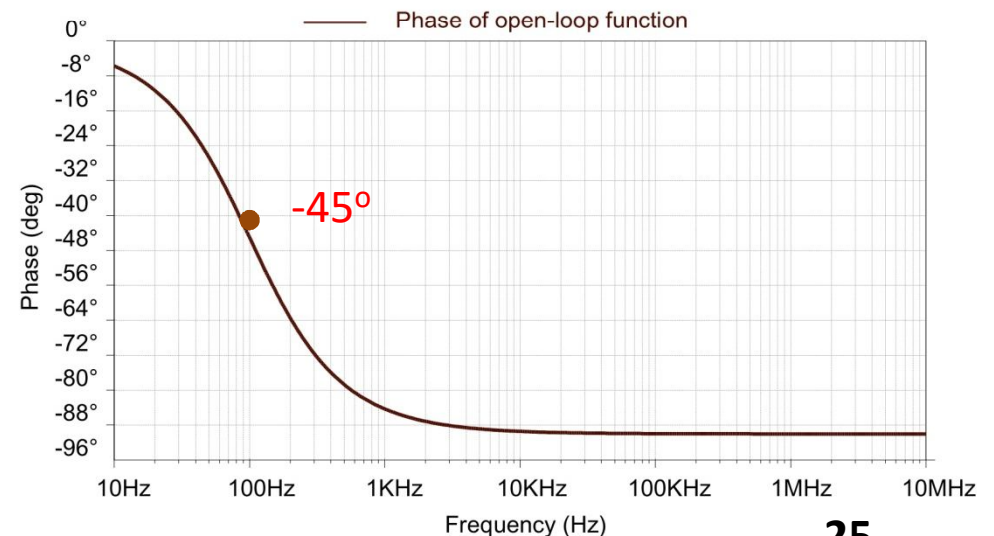
Bode plots of open-loop function



Nyquist plot of open-loop function



Nyquist chart



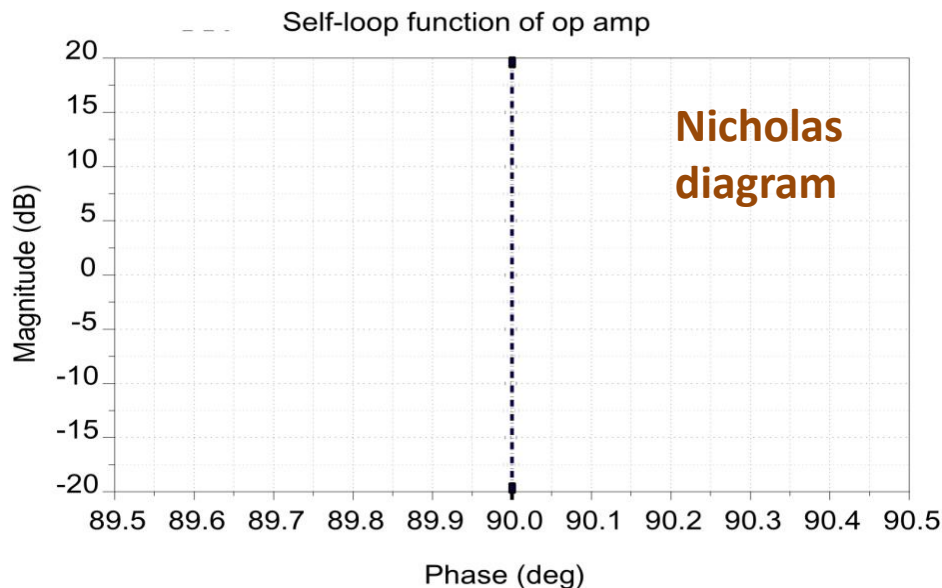
2. Analysis of High-Order Transfer Functions

Behavior of Self-loop Function of Ideal Op Amp

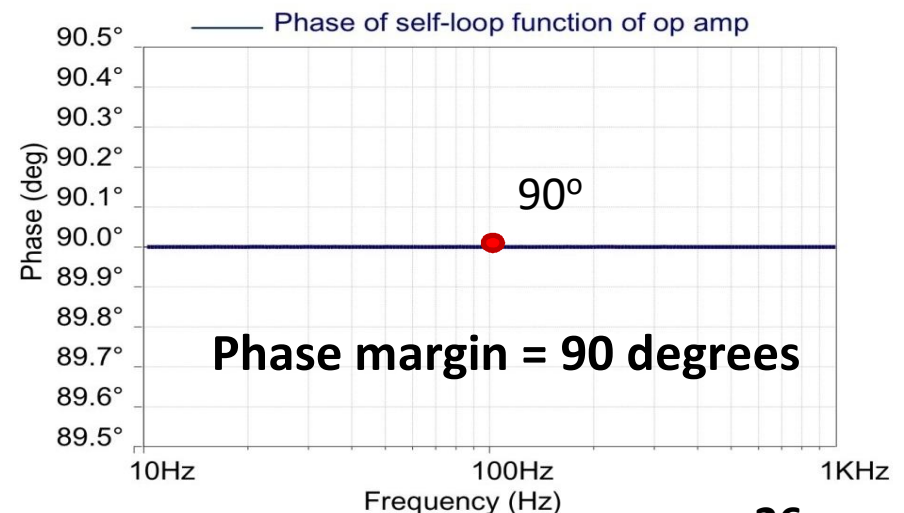
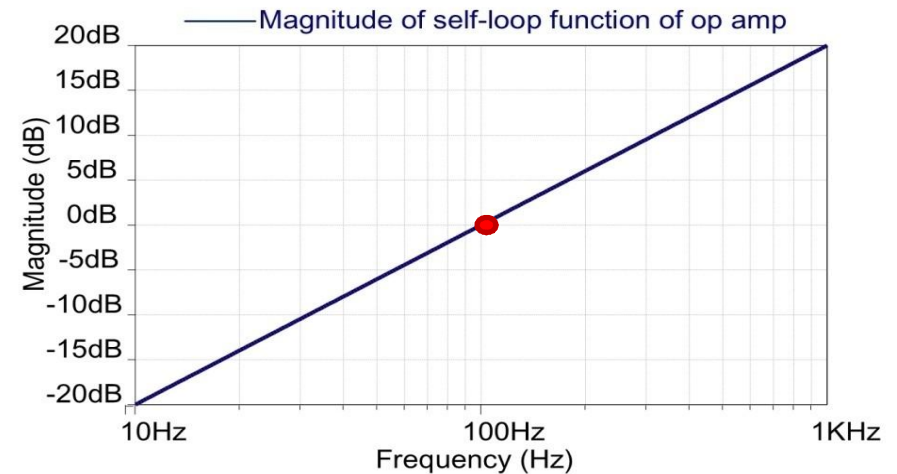
Self-loop function $L(\omega)$

$$L(\omega) = j \frac{\omega}{200\pi} = 10^5 \frac{V_{in}}{V_{out}} - 1$$

Magnitude-angular plot of self-loop function



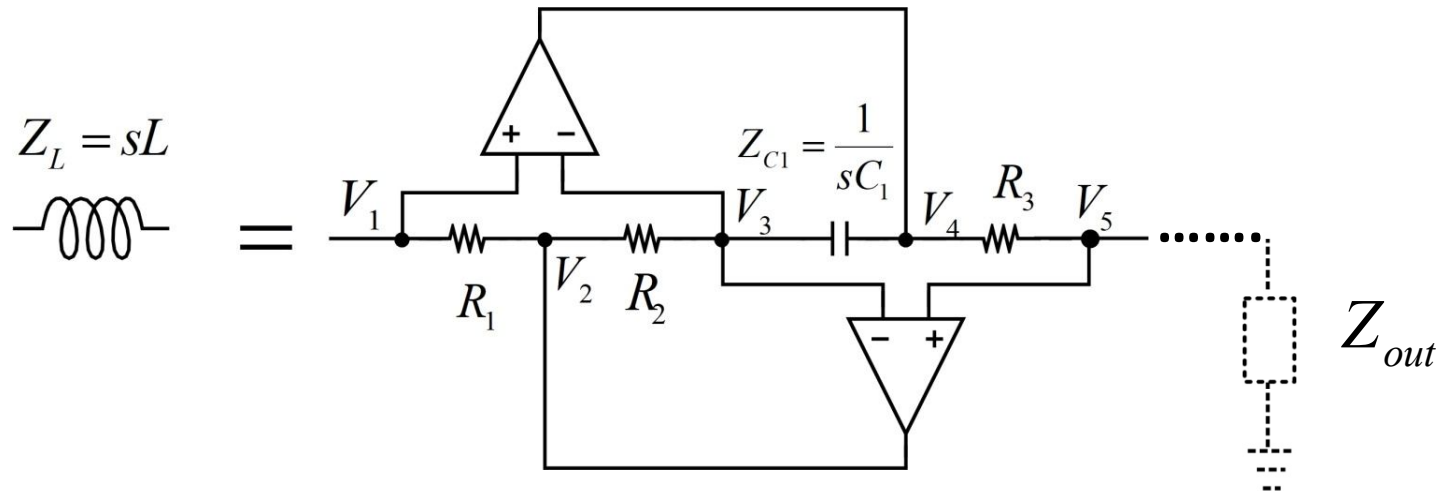
Bode plots of self-loop functions



2. Analysis of High-Order Transfer Functions

Analysis of Active Inductor

General impedance converter



Apply superposition principle at V3

$$V_3 \left(\frac{1}{R_2} + \frac{1}{Z_C} \right) = \frac{V_2}{R_2} + \frac{V_4}{Z_C} \quad \text{Here, } V_1 = V_3 = V_5$$

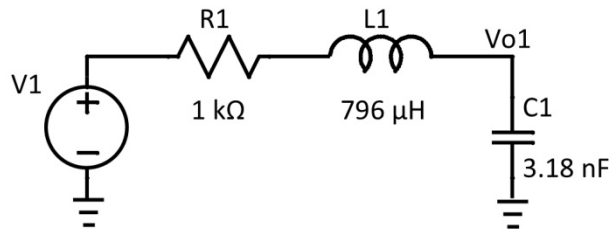
Approximated value of active inductor

$$Z_L = \frac{R_2}{R_1} \frac{R_3}{Z_C} Z_{out} = \frac{R_2 R_3}{R_1} s C Z_{out}$$

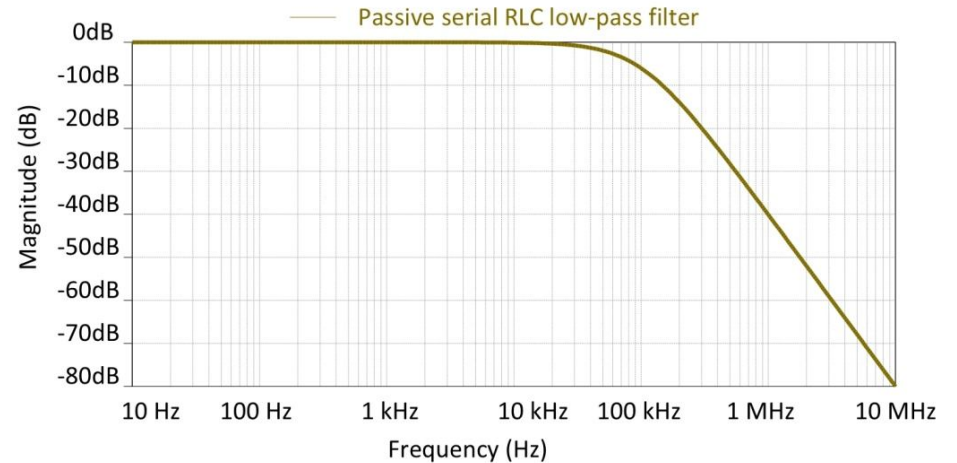
2. Analysis of High-Order Transfer Functions

Simulations of Passive & Active RLC Low-pass Filters

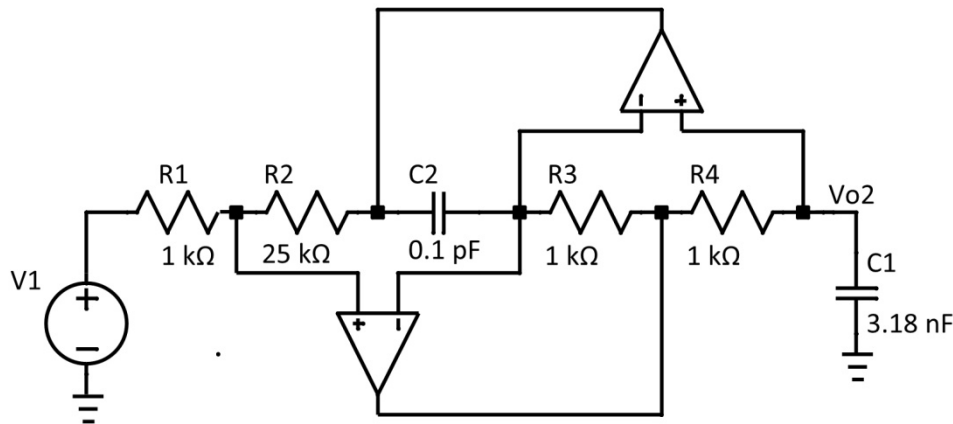
Passive serial RLC Low-pass Filter



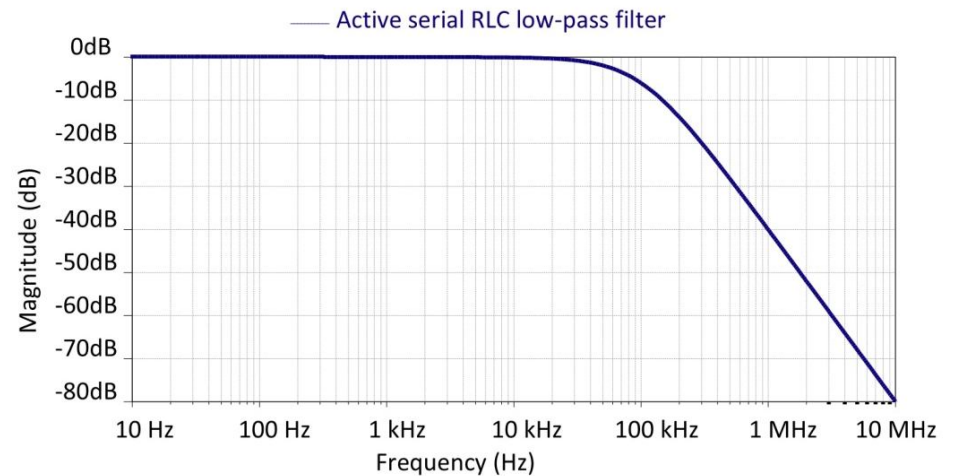
Magnitude response of transfer function



Active serial RLC Low-pass Filter



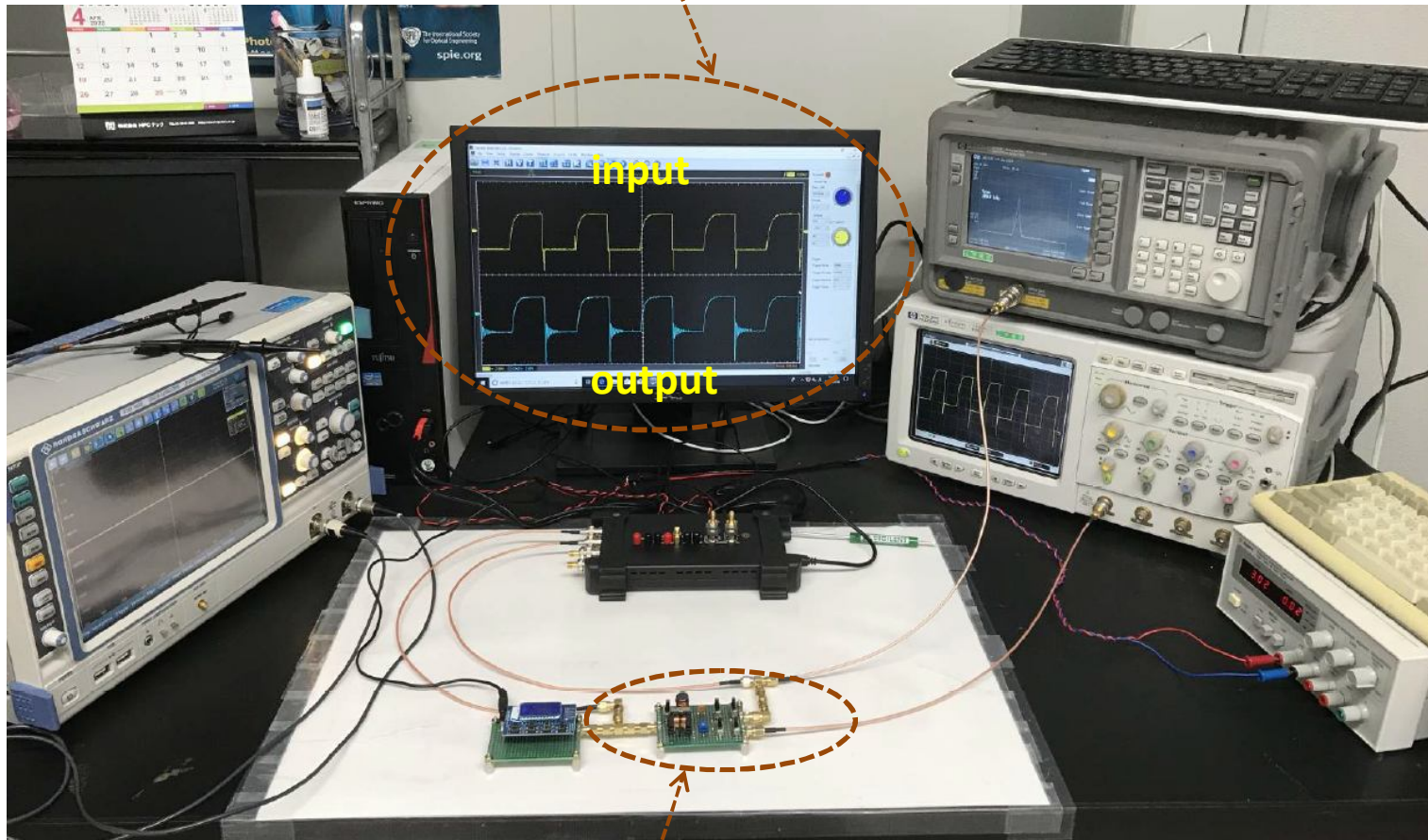
Magnitude response of transfer function



3. Proposed Designs and Experimental Results

Implementation of Second-order Serial RLC LPF

Under-shoot occurred at both input and output ports.

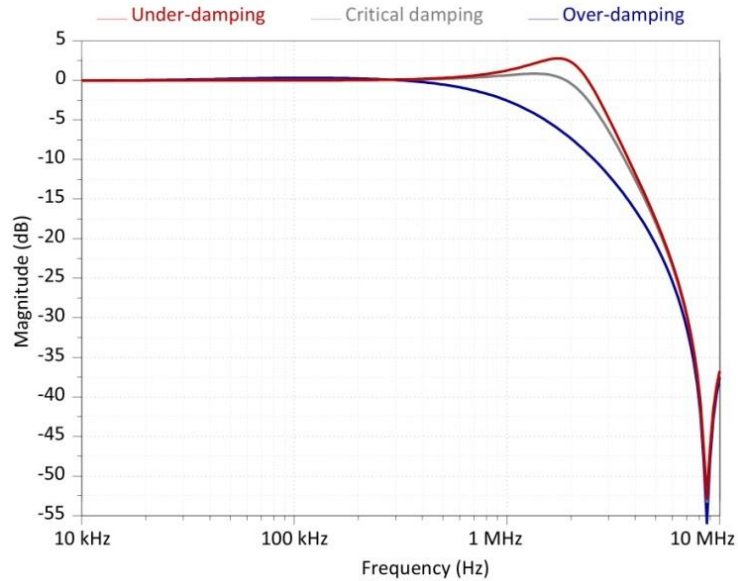


Device under test

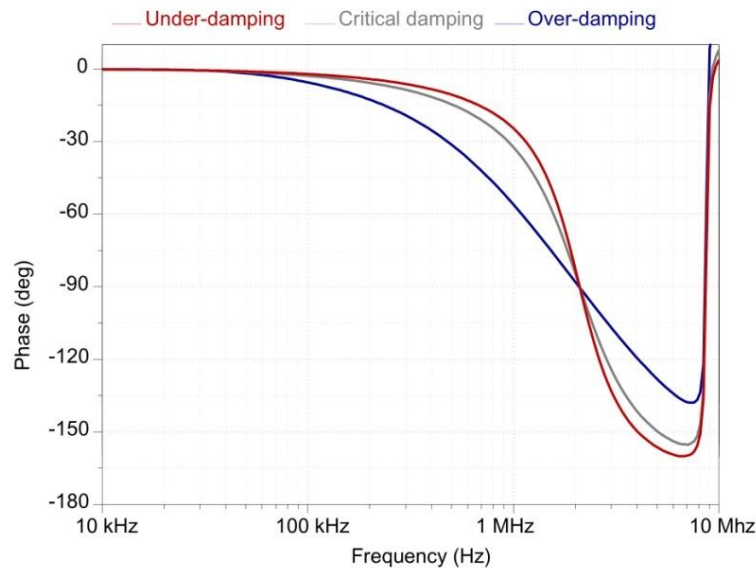
3. Proposed Designs and Experimental Results

Measured Transfer Function in Serial RLC LPF

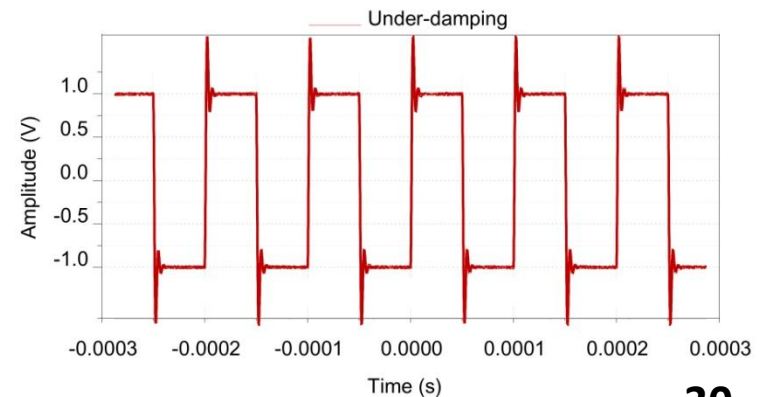
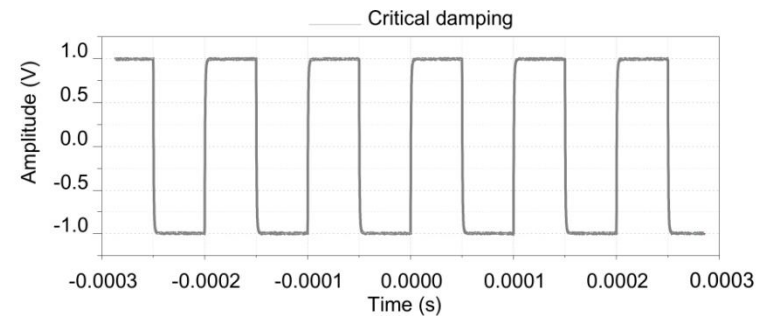
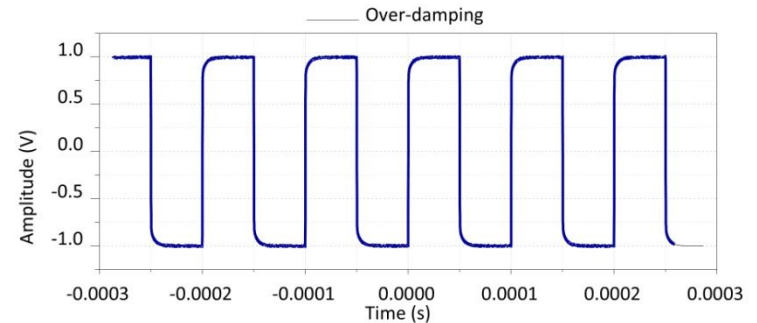
Magnitude response



Phase response



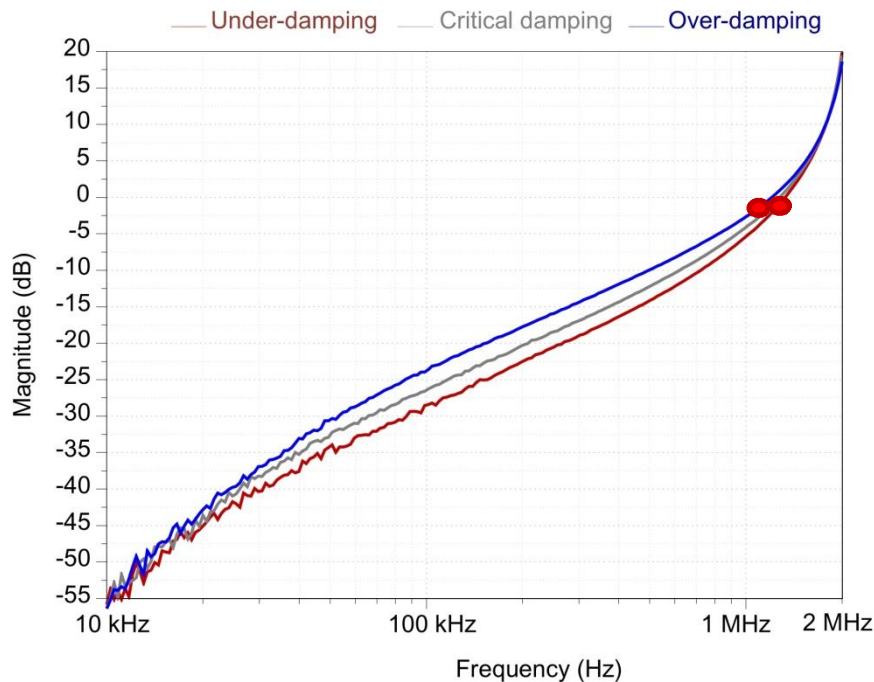
Transient response



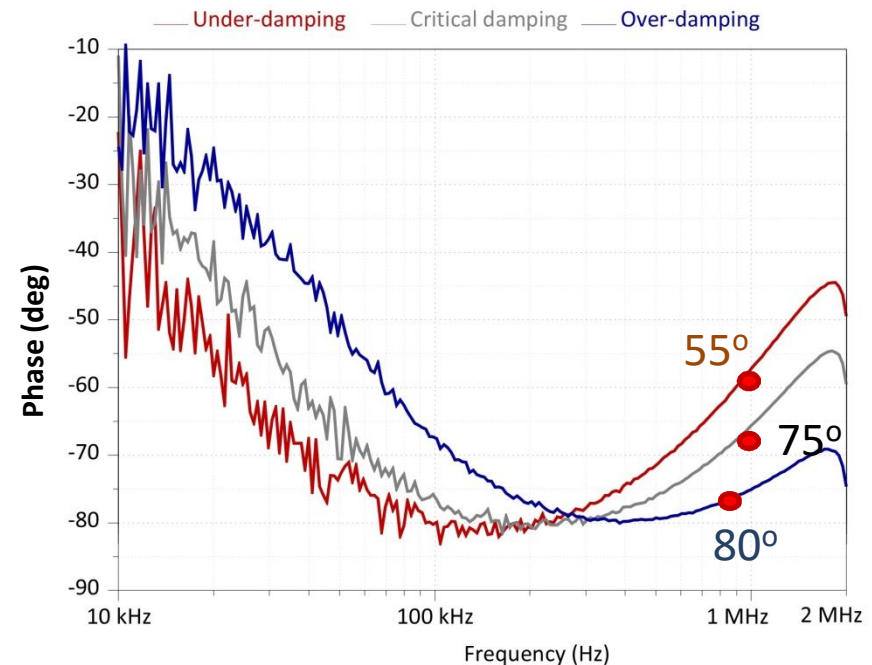
3. Proposed Designs and Experimental Results

Measured Self-loop Function in Serial RLC LPF

Magnitude response



Phase response



Over-damping: → Phase margin is 80 degrees.

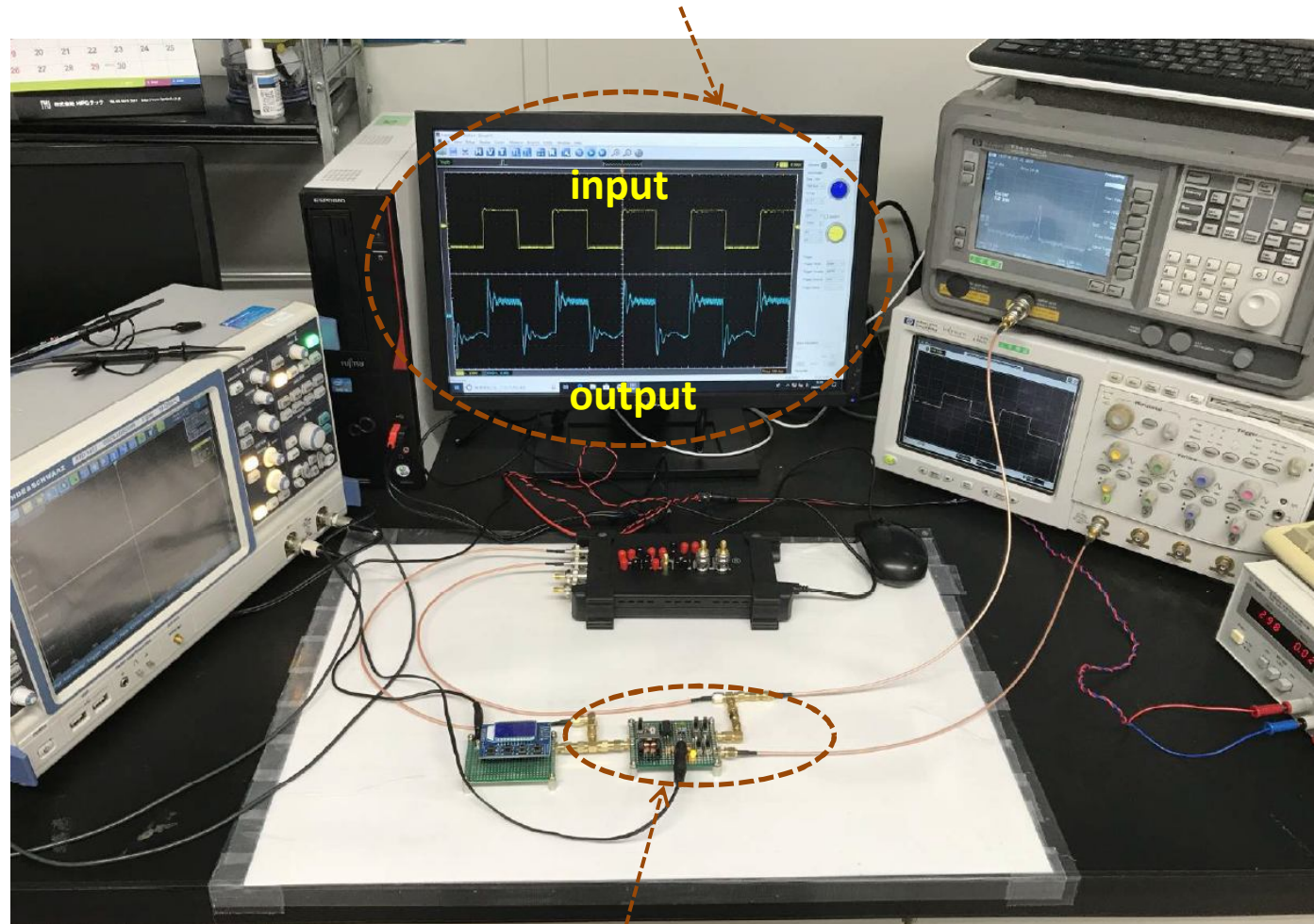
Nearly Critical damping: → Phase margin is 75 degrees.

Under-damping: → Phase margin is 55 degrees.

3. Proposed Designs and Experimental Results

Implementation of Active RLC Low-pass Filter

Over-shoot occurred at output port.

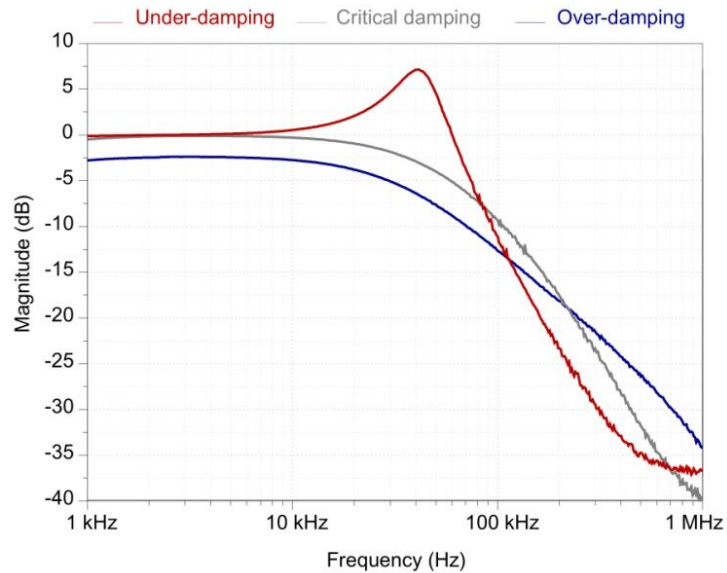


Device under test

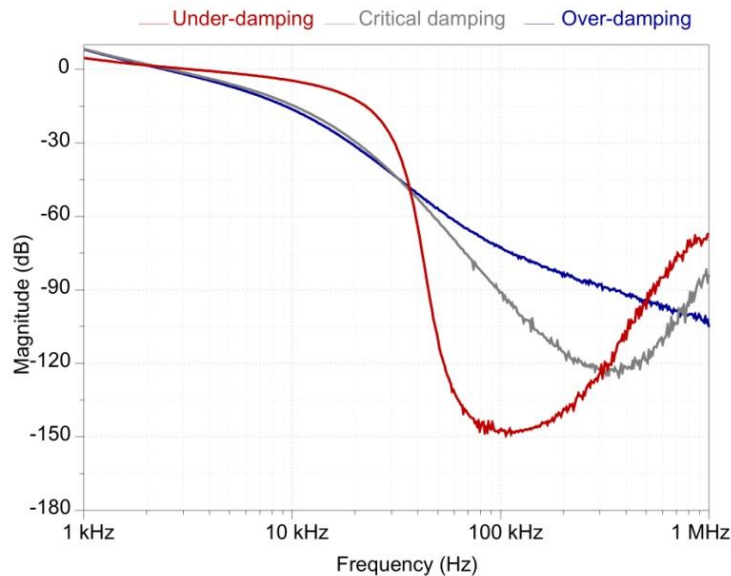
3. Proposed Designs and Experimental Results

Measured Transfer Function of Active RLC LPF

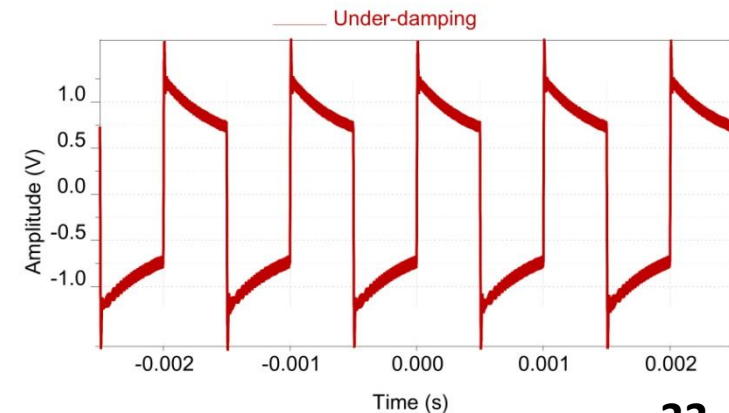
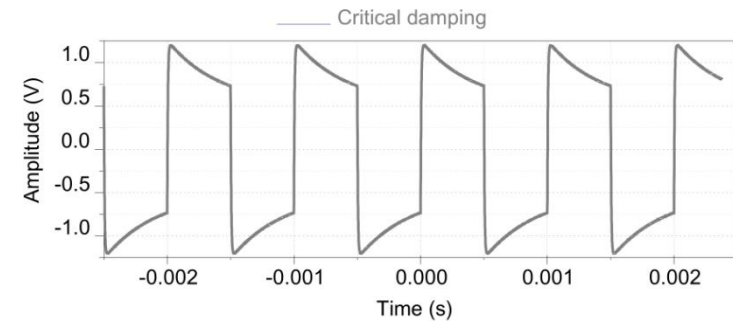
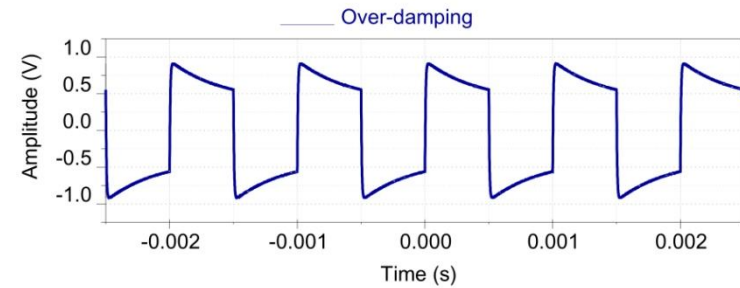
Magnitude response



Phase response



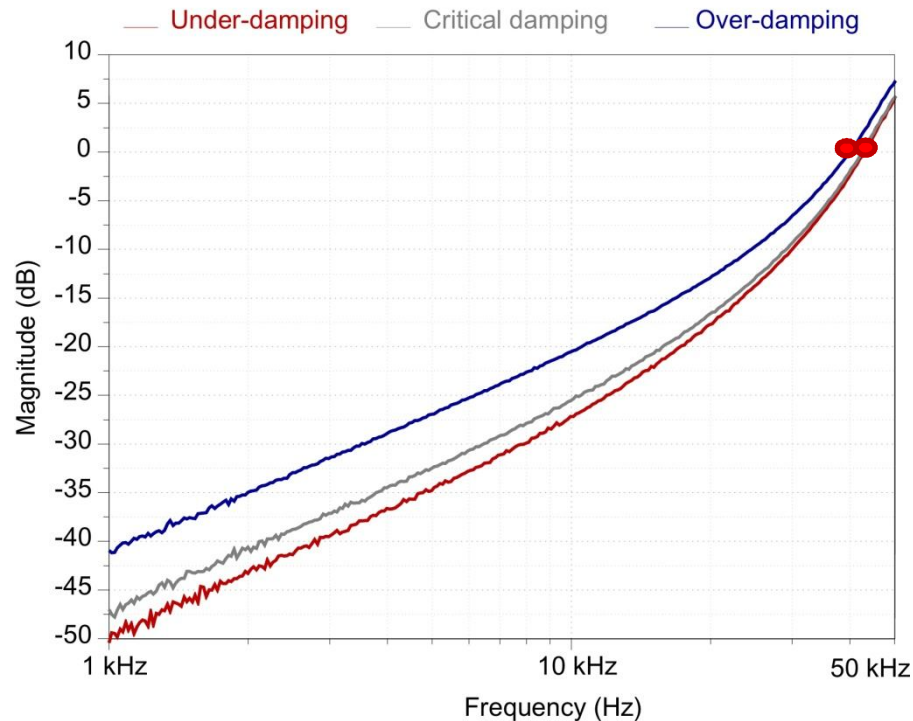
Transient response



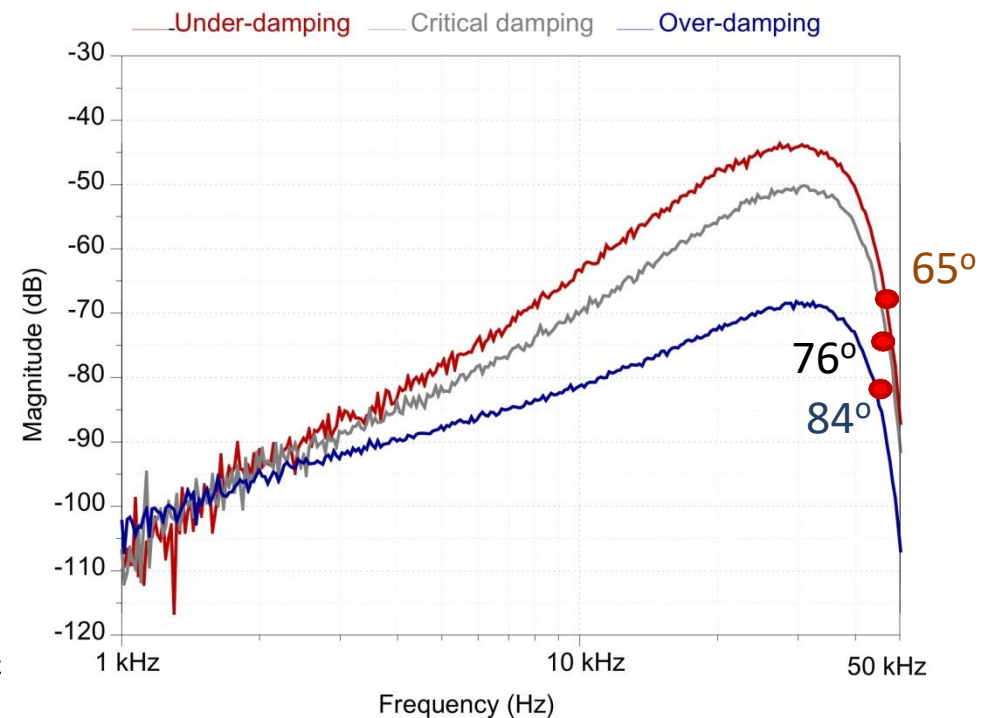
3. Proposed Designs and Experimental Results

Measured Self-loop Function of Active RLC LPF

Magnitude response



Phase response



Over-damping: → Phase margin is 84 degrees.

Nearly Critical damping: → Phase margin is 76 degrees.

Under-damping: → Phase margin is 65 degrees.

4. Conclusions



This work:

- **Reviews of complex functions and stability test**
- **Proposed methods for derivation of transfer function and measurement of self-loop function**
- **Implementations and measurements of self-loop functions for passive and active second-order RLC low-pass filters**
- **Theoretically, if phase margin is smaller than 76.3-degrees, overshoot occurs in second-order systems.**

Future of work:

- **Stability test for polyphase filters & complex filters**

References



- [1] H. Kobayashi, N. Kushita, M. Tran, K. Asami, H. San, A. Kuwana "Analog - Mixed-Signal - RF Circuits for Complex Signal Processing", IEEE 13th International Conference on ASIC (ASICON 2019) Chongqing, China (Nov, 2019).
- [2] M. Tran, C. Huynh, "A Design of RF Front-End for ZigBee Receiver using Low-IF Architecture with Poly-phase Filter for Image Rejection", M.S. thesis, University of Technology Ho Chi Minh City – Vietnam (Dec. 2014).
- [3] H. Kobayashi, M. Tran, K. Asami, A. Kuwana, H. San, "Complex Signal Processing in Analog, Mixed - Signal Circuits", Proceedings of International Conference on Technology and Social Science 2019, Kiryu, Japan (May. 2019).
- [4] M. Tran, N. Kushita, A. Kuwana, H. Kobayashi "Flat Pass-Band Method with Two RC Band-Stop Filters for 4-Stage Passive RC Quadratic Filter in Low-IF Receiver Systems", IEEE 13th ASICON 2019 Chongqing, China (Nov. 2019).
- [5] M. Tran, Y. Sun, N. Oiwa, Y. Kobori, A. Kuwana, H. Kobayashi, "Mathematical Analysis and Design of Parallel RLC Network in Step-down Switching Power Conversion System", Proceedings of International Conference on Technology and Social Science (ICTSS 2019) Kiryu, Japan (May. 2019).
- [6] M. Tran, "Damped Oscillation Noise Test for Feedback Circuit Based on Comparison Measurement Technique", 73rd System LSI Joint Seminar, Tokyo Institute of Technology, Tokyo, Japan (Oct. 2019).
- [7] R. Middlebrook, "Measurement of Loop Gain in Feedback Systems", Int. J. Electronics, Vol 38, No. 4, pp. 485-512, (1975).
- [8] M. Tran, Y. Sun, Y. Kobori, A. Kuwana, H. Kobayashi, "Overshoot Cancellation Based on Balanced Charge-Discharge Time Condition for Buck Converter in Mobile Applications", IEEE 13th ASICON 2019 Chongqing, China (Nov, 2019).
- [9] A. Sedra, K. Smith (2010) Microelectronic Circuits 6th ed. Oxford University Press, New York.
- [10] R. Schaumann, M. Valkenberg, (2001) Design of Analog Filters, Oxford University Press.
- [11] B. Razavi, (2016) Design of Analog CMOS Integrated Circuits, 2nd Edition McGraw-Hill.
- [12] M. Tran, N. Miki, Y. Sun, Y. Kobori, H. Kobayashi, "EMI Reduction and Output Ripple Improvement of Switching DC-DC Converters with Linear Swept Frequency Modulation", IEEE 14th International Conference on Solid-State and Integrated Circuit Technology, Qingdao, China (Nov. 2018).
- [13] J. Wang, G. Adhikari, N. Tsukiji, M. Hirano, H. Kobayashi, K. Kurihara, A. Nagahama, I. Noda, K. Yoshii, "Equivalence Between Nyquist and Routh-Hurwitz Stability Criteria for Operational Amplifier Design", IEEE International Symposium on Intelligent Signal Processing and Communication Systems (ISPACS), Xiamen, China (Nov. 2017).

6th International Conference on Signal and Image Processing (SIPRO 2020)

July 25-26, 2020, London, United Kingdom



Thank you very much!

